THE JOURNAL OF PHYSICAL CHEMISTRY LETTERS
A JOURNAL OF THE AMERICAN CHEMICAL SOCIETY

pubs.acs.org/JPCL

Letter

Electrocatalytic Activity of Polyaniline in Magnesium−Sulfur Batteries

Murali Krishna, Arnab Ghosh, Divyamahalakshmi Muthuraj, Sharmistha Das, and Sagar Mitra*

Cite This: *J. Phys. Chem. Lett.* 2022, 13, 1337−1343

Read Online

ACCESS | Metrics & More | Article Recommendations | Supporting Information

ABSTRACT: Rechargeable magnesium−sulfur (Mg−S) batteries offer the potential for inexpensive energy storage alternatives to other metal-ion batteries for the grid scale and household applications. Despite all economic and resource advantages, Mg−S battery chemistry suffers from a complicated reaction mechanism and extremely slow reaction kinetics. To improve the kinetics, we improvise a new electrode architecture where a conductive polymer is used along with a carbon network. This report will bring an important insight of electrocatalytic activity of polyaniline, on the basis of free-radical coupling and is a completely new concept in Mg−S battery chemistry. By the combined electron spin resonance spectroscopy, X-ray photoelectron spectroscopy, and fluorescence lifetime measurements, we perceived that the polyaniline anchors the $S_3^{\bullet-}$ species from the electrolyte/catholyte through a free-radical-coupling process and thus promotes the reduction to end-discharged products, via a chemical adduct. The concept of free-radical catalysis in Mg/S batteries will open a new knowledge to enhance the active material utilization in the Mg−S batteries.

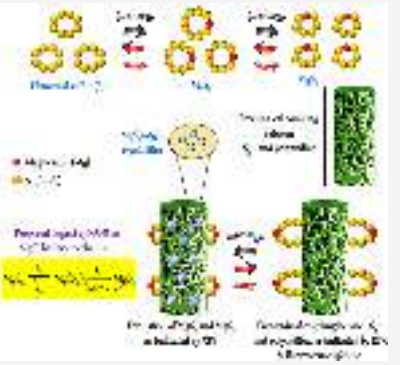

Rechargeable magnesium−sulfur (Mg−S) batteries are considered as a class of low-cost energy storage option in near future. The duo of magnesium (Mg) and sulfur (S) together offer a high theoretical volumetric energy density of 3200 Wh L^{-1}.[1] Moreover, due to its lower diffusion barrier (at lower current density) and higher-coordinated configurations,[2] Mg is less susceptible to formation of metallic dendrites than Li, hence substantially improving the safety of Mg−S batteries. Despite considerable benefits, a successful demonstration of practical Mg−S batteries is being hindered due to their low practical cell capacity, mainly arising from exceptionally sluggish kinetics associated with redox conversion of elemental sulfur (S_8) against Mg, magnesium anode passivation, lack of electrolyte compositions, and rapid dissolution of intermediate polysulfides into the ether-based electrolytes.[1,3,4]

A promising way to mitigate these challenges simultaneously lies in either modification of electrolytes[1,5−10] or fabrication of efficient sulfur cathodes.[11−14] Kim et al. reported the first non-nucleophilic electrolyte, compatible with both S and Mg.[1] 1-Butyl-1-methylpiperidinium bis(trifluoromethylsulfonyl)imide ($PP_{14}TFSI$) ionic liquid was used as an electrolyte additive to reduce the polysulfide shuttling by enhancing the viscosity of the electrolyte.[6] An electrolyte containing a boron-centered anion-based salt helped to improve the cycle life of Mg−S batteries.[5] Furthermore, in order to promote the kinetics of Mg−S chemistry, the concept of using a Li^+ mediator in the electrolyte was also documented.[8] However, in parallel to the electrolyte modifications, preparation of effective sulfur-based composite cathodes was also found to enhance the electrochemical performance of Mg−S cell. Fichtner et al. synthesized a graphene-based sulfur nanocomposite cathode that delivered an initial reversible specific capacity of 448 mA h g^{-1} and retained to 236 mA h g^{-1} after 50 cycles.[11] From our group, a cathode made of drop-casted sulfur/reduced graphene oxide (S/rGO) nanocomposite on N,S dual-doped carbon cloth current collector was proposed.[13] The cathode that exhibited a stable cycling performance of 40 cycles through suppression of the polysulfide dissolution phenomenon and shuttling behavior in Mg−S cell.[13] In addition, we have recently reported the utility of a liquid-phase magnesium-polysulfide (MgS_x) catholyte as an active material in Mg−S batteries.[14] The MgS_x catholyte was loaded on a polyaniline-coated carbon cloth (CC@PANI) current collector. Due to hydrophilic nature of polyaniline, it effectively immobilized the electrolyte-soluble MgS_x species, and thus the cycle life of Mg−S was improved. In this work, the CC@PANI current collector soaked with the liquid-phase MgS_x catholyte (abbreviated as CC@PANI@MgS_x cathode) delivers a reversible specific capacity of 510 mA h g^{-1} at second cycle and retains a high reversible capacity of 495 mA h g^{-1} (i.e., ∼97% of initial reversible capacity) after 30 cycles. However, apart from improvement of the cycling stability, polyaniline-coated

Received: December 10, 2021
Accepted: February 1, 2022
Published: February 2, 2022

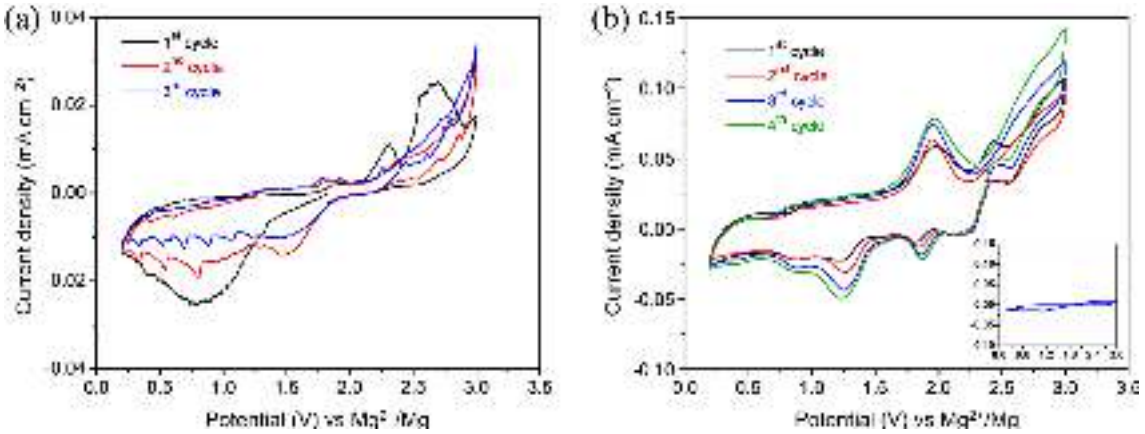

Figure 1. (a) Cyclic voltammetry (CV) profiles of the CC@MgS_x cathode at 0.02 mV s^{-1} and (b) CV profiles of the CC@PANI@MgS_x cathode at 0.02 mV s^{-1}. The inset shows the CV curve of the CC@PANI current collector at 0.02 mV s^{-1}.

electrode substantially enhances the utilization of active materials, as observed from the appearance of several new redox peaks with good reversibility and repeatability in the cyclic voltammetry curves.

In this continuation, we have investigated the electrocatalytic activity of polyaniline in Mg−S batteries utilizing electron spin resonance spectroscopy (ESR), X-ray photoelectron spectroscopy (XPS), and fluorescence lifetime imaging microscopy (FLIM). The ESR and XPS analyses indicate that polyaniline catalyzes the redox conversion of Mg-polysulfide radical-monoanions to the lower-order Mg-sulfides through a radical-coupling reaction, which is further supported by fluorescence lifetime measurements. The current investigation is new for Mg−S battery chemistry and can excavate a common methodology to design sustainable sulfur-based cathode architectures with different electrocatalytic additives.

Like alkali metal−sulfur (e.g., Li/S, Na/S) batteries, magnesium−sulfur (Mg/S) batteries also suffer from poor electrochemical kinetics and severe shuttle phenomenon associated with fast dissolution of polysulfides into liquid electrolyte. All of these technical issues synergistically lead to low specific cell capacity, inferior cycle life, and poor Coulombic efficiency. It is believed that all of the issues can be significantly resolved through incorporation of catalytic substrates/additives into the battery electrode. Although several reports of catalytic effects on the electrochemical characteristics of Li/S and Na/S batteries have been reported until date,[15−18] no such prominent catalytic activities in Mg/S batteries are illustrated until date. Here the electrocatalytic activity of polyaniline (PANI) in Mg/S batteries has been investigated and proposed through ESR spectroscopy and XPS characterization, as discussed in the following section.

The emeraldine salt of polyaniline was synthesized and deposited on the surface of carbon cloth via an in situ chemical polymerization route in the presence of ammonium persulfate as an oxidant and sulfuric acid as a protonic acid dopant. The successful formation of polyaniline was confirmed by the X-ray photoelectron spectroscopy (XPS) characterization technique. The deconvoluted C(1s) XPS spectrum of polyaniline-coated carbon cloth (CC@PANI) exhibits three characteristic peaks (Figure S1a). The C(1s) XPS peak centered at the binding energy of 284.5 eV can be attributed to the phenyl groups present in polyaniline and the graphitic carbons of carbon cloth. The characteristic C(1s) XPS peak of the polysemiquinone radical-cations (i.e., C−$N^{+\bullet}$−H moiety) can be observed at the binding energy of 285.8 eV, suggesting formation of a polaron in the polyaniline. The broad peak component centered at the binding energy of 287.8 eV arises due to carboxylic groups, which are plausibly generated on the surface of carbon cloth during the chemical treatment. Furthermore, the deconvoluted N(1s) spectrum exhibits three characteristic peaks of the quinoid amine (399.4 eV), polysemiquinone radical-cations (400.5 eV), and iminium ions (402.0 eV), respectively[19] (Figure S1b). The microstructure and morphology of the CC@PANI substrate were investigated through the scanning electron microscopy (SEM) characterization technique. SEM images of the CC@PANI reveal uniform growth of a polyaniline layer on the surface of the carbon fibers (Figure S1c). The high-resolution SEM image indicates a porous morphology of the polyaniline layer (Figure S 1d), which might be beneficial to increase the electrolyte/catholyte accessibility. Besides, the homogeneous characteristic of the as-grown polyaniline layer might offer enormous binding sites to immobilize the higher-order Mg-polysulfides.

To observe the electrocatalytic activity of polyaniline, two different electrodes were fabricated by loading the MgS_x catholyte on pristine carbon cloth (CC) and polyaniline-coated carbon cloth (CC@PANI) and cycling against Mg anode. Figure 1 panels a and b represent the cyclic voltammetry (CV) curves of the CC@MgS_x cathode and CC@PANI@MgS_x cathode, respectively. Both Mg/S cells, containing the MgS_x@CC cathode and MgS_x@CC@PANI cathode separately, were subjected to an initial cathodic scan from their respective open circuit potential. During the initial cathodic scan, the CC@MgS_x cathode manifested a broad reduction peak within the voltage range 1.35−0.5 V (vs Mg^{2+}/Mg), which might be attributed to electrochemical conversion of MgS_x to end-discharged product as per previous report.[14] In subsequent anodic scan, the CC@MgS_x cathode displayed two characteristic peaks corresponding to two-step oxidation of end-discharged product to elemental sulfur.[11,14] During the second scan, although the CC@MgS_x cathode repeatedly exhibited the characteristic reduction peak, no obvious oxidation peak was noticed, suggesting a less feasible Mg^{2+} extraction process. In contrast to the CC@MgS_x cathode, CV profiles of the CC@PANI@MgS_x cathode reveal the multiple redox peaks with higher current density values (Figure 1b), indicating a large mass transfer process at the electrode interface. During the initial cathodic scan, the CC@PANI@MgS_x cathode exhibited the first reduction peak at 1.82 V,

https://doi.org/10.1021/acs.jpclett.1c04021
J. Phys. Chem. Lett. 2022, 13, 1337−1343

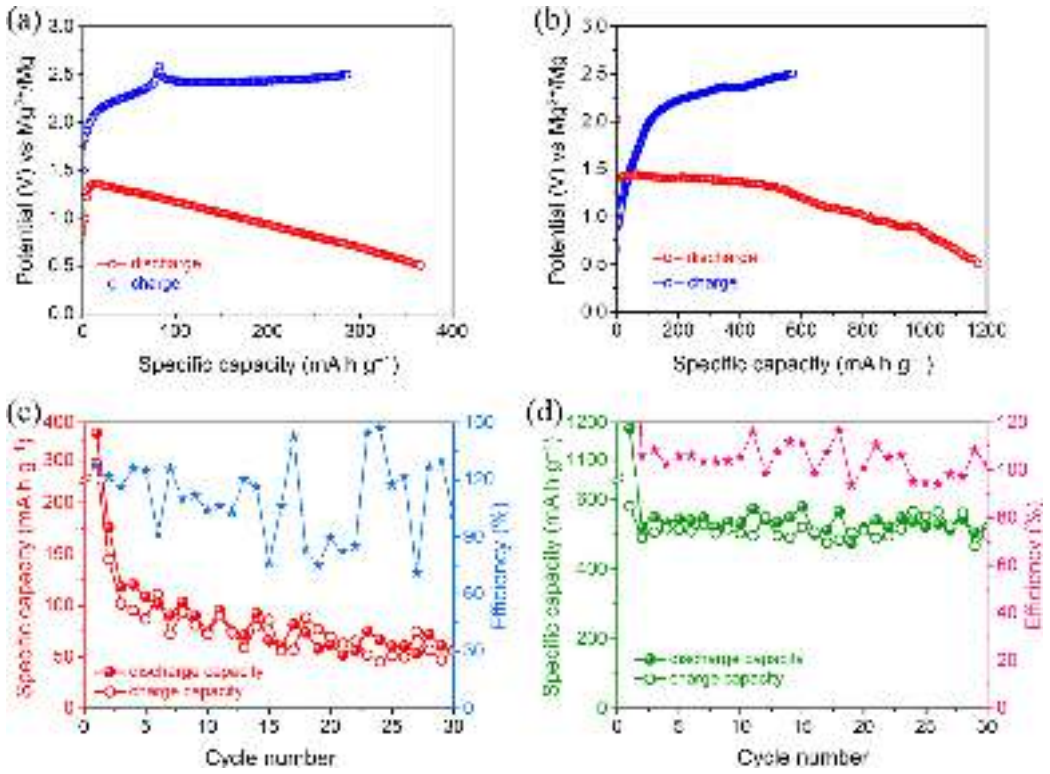

Figure 2. (a, b) First cycle galvanostatic charge/discharge profiles of the CC@MgS_x cathode (a) and the CC@PANI@MgS_x cathode (b) and (c, d) cycling performance of the CC@MgS_x cathode (c) and the CC@PANI@MgS_x cathode (d) at the 20 mA g^{-1} current rate.

followed by a broad reduction peak (second reduction peak) located at 1.25 V (vs Mg^{2+}/Mg). The last (third) reduction peak can be observed within the potential range 1.0−0.7 V (vs Mg^{2+}/Mg). During anodic scan of the CC@PANI@MgS_x cathode, two oxidation peaks were observed. The first oxidation peak locates within the potential range 1.75−2.3 V, while the second oxidation peak appears within the range 2.40−3.0 V (vs Mg^{2+}/Mg), corresponding to complete conversion of Mg-polysulfides back to elemental sulfur. The appearance of additional redox peaks indicates the catalytic activities in the CC@PANI@MgS_x cathode. Interestingly, the CC@PANI@MgS_x cathode maintained the repeatability of each redox peak during the CV scans. It is noteworthy to emphasize that the CC@PANI current collector did not participate in the electrochemical reaction within the working potential range 0.2−3.0 V (vs Mg^{2+}/Mg) and therefore did not contribute to the specific capacity of the Mg/S batteries (inset, Figure 1b).

Figure 2a represents first cycle galvanostatic charge/discharge profile of the CC@MgS_x cathode at a current rate of 20 mA g^{-1}. The discharge profile exhibits an inclined plateau within the potential range 1.35−0.5 V, well-resembling to the broad reduction peak observed within the similar potential range during cathodic scan. In contrast, the first cycle charge/discharge profiles of the CC@PANI@MgS_x cathode display multiple plateaus (Figure 2b), which well-resemble the multiple redox peaks observed in the CV profiles. The charge/discharge cycling performance of the CC@MgS_x cathode and the CC@PANI@MgS_x cathode, within a potential window of 0.5−2.5 V, is shown in Figure 2c,d. The CC@MgS_x cathode delivered an initial specific discharge capacity of 372 mA h g^{-1} and a subsequent charge capacity of 288 mA h g^{-1}, corresponding to the initial Coulombic efficiency of ∼77.4% (Figure 2c). After the first cycle of charge/discharge, the CC@MgS_x cathode exhibited a specific discharge capacity of 177 mA h g^{-1} and a specific charge capacity of 142 mA h g^{-1} at the second cycle, corresponding to a Coulombic efficiency of ∼80.2% (Figure 2c). From the third cycle onward, although the CC@MgS_x cathode experienced improved average Coulombic efficiency over 90%, the cycling stability appears to be inferior. The inferior cycling stability of the CC@MgS_x cathode might be ascribed to the inefficiency of the hydrophobic surface of pristine carbon cloth to immobilize the electrolyte-soluble higher-order MgS_x ($8 \geq x \geq 4$) species during charge/discharge operation of the Mg/S batteries. The readily dissolved higher-order MgS_x moieties diffuse toward the Mg metal anode and chemically react to form an electrolyte-insoluble, insulating layer of lower-order Mg-sulfides (MgS_2/MgS). The mixed phase of insulating lower-order Mg-sulfides gradually precipitates and covers the surface of the Mg anode, which hampers the facile Mg^{2+} transportation between the electrolyte and the Mg anode and thus results in low practical capacity. However, the CC@PANI@MgS_x cathode demonstrated very stable cycling behavior with excellent Coulombic efficiencies (Figure 2d). Delivering a reversible specific capacity of 510 mA h g^{-1} at the second cycle, the CC@PANI@MgS_x cathode retained as much as high reversible capacity of 495 mA h g^{-1} (i.e., ∼97% of initial reversible capacity) after 30 cycles. For the CC@PANI@MgS_x cathode, the excellent cycling performance along with the appearance of several redox peaks with good reversibility/repeatability could be attributed to the effective entrapment of polysulfides by the CC@PANI current collector as well as the electrocatalytic activity of polyaniline that propels the conversion of electrolyte-soluble higher-order Mg-polysulfides

https://doi.org/10.1021/acs.jpclett.1c04021
J. Phys. Chem. Lett. 2022, 13, 1337−1343

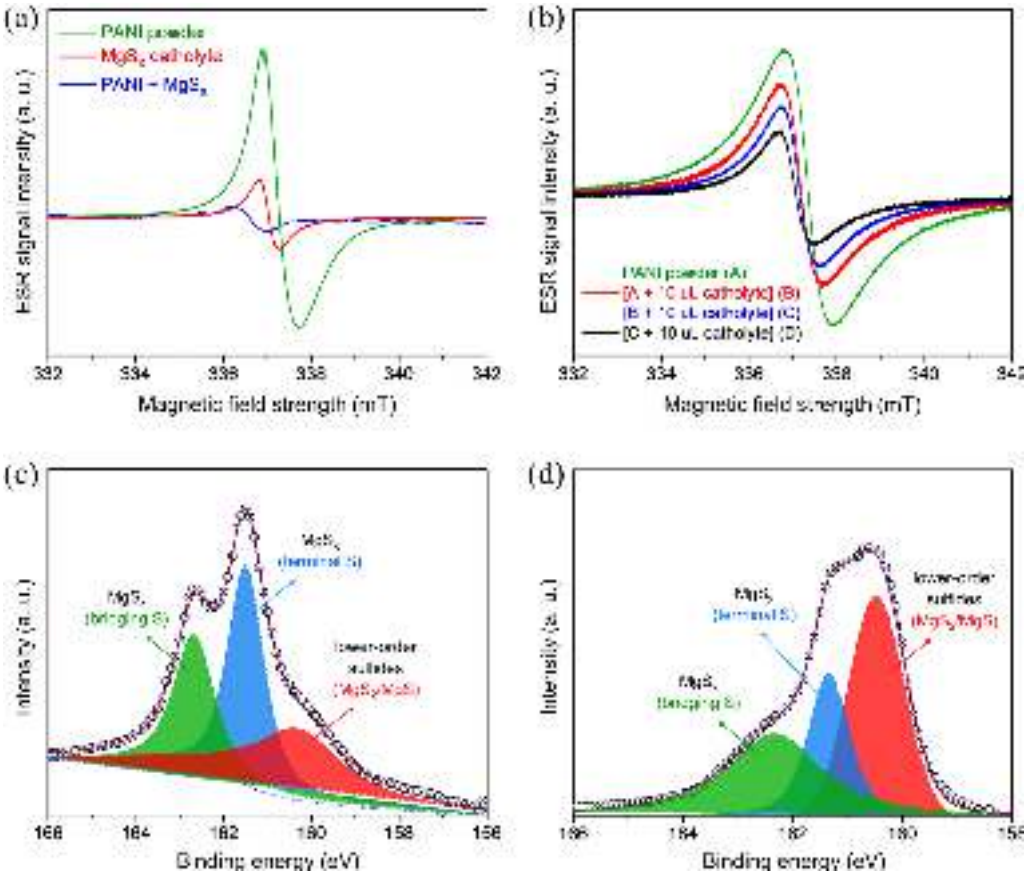

Figure 3. (a) ESR spectra of the individual polyaniline powder, the MgS_x catholyte, and their mixture. (b) ESR spectra recorded on polyaniline powder during continuous addition of the MgS_x catholyte. (c, d) Deconvoluted S $2p_{3/2}$ XPS spectra of the CC@MgS_x cathode and the CC@PANI@MgS_x cathode after complete discharge.

(MgS_x, $8 \geq x \geq 3$) to insoluble lower-order Mg-sulfides (MgS_2/MgS).

Polyaniline emeraldine salt (PANI-ES), the conducting form of polyaniline, is synthesized through doping the emeraldine base (nonconducting form) by protonic acids. An excellent electronic conductivity of polyaniline is observed and mainly attributed to the protonated nitrogen radical-atoms (also known as nitrogen-centered radical-cations) in the polaronic segments that appear to have extended π-delocalization in the polymer backbone.[20−22] However, these nitrogen-centered radical-cations are highly susceptible toward the radical-coupling reaction to form phenazine-like rings.[23−25] Besides, metal−sulfur batteries are well-known to go through different intermediates, including polysulfide dianions (S_n^{2-}) and trisulfur radical-monoanions ($S_3^{\bullet-}$).[26−29] Therefore, it is plausible that polyaniline involves the process of radical coupling with $S_3^{\bullet-}$ species and eventually facilitates their redox conversion to end-discharge products. To validate this hypothesis, the MgS_x catholyte was characterized by Raman spectroscopy to first detect the existence of $S_3^{\bullet-}$ species. The deconvoluted Raman spectrum of the MgS_x catholyte reveals the characteristic bands of unreacted S_8 and MgS,[30] polysulfide dianions (S_n^{2-}, $8 \geq n \geq 4$),[29−31] and $S_3^{\bullet-}$ radical-monoanions[32] (Figure S2a). Furthermore, the UV−visible spectrum acquired on the MgS_x catholyte displays typical absorption peaks at 417, 482, and 670 nm, corresponding to S_6^{2-}, S_4^{2-}, and $S_3^{\bullet-}$ species, respectively[14] (Figure S2b).

Electron spin resonance (ESR) spectroscopy was further employed to investigate the formation of polaronic segments containing nitrogen-centered radical-cations in our as-prepared polyaniline grown on the surface of carbon cloth as well as to further confirm the existence of polysulfide radical-monoanions in the MgS_x catholyte. Figure 3a represents the ESR spectra of the individual polyaniline (PANI) powder, the MgS_x catholyte, and their mixture. The sharp ESR signal of PANI powder confirms the generation of polaronic segments in the polymer chain (polysemiquinone radical-cations). The strong ESR signal of the MgS_x catholyte further suggests that the polysulfide dianions tend to undergo a disproportionation reaction to generate paramagnetic polysulfide radical-monoanions through the aprotic solvents with high donor numbers (such as TEGDME). Interestingly, the mixture of two individual paramagnetic samples (i.e., PANI powder and MgS_x catholyte) shows a suppressed ESR signal, indicating a plausible radical-coupling process. To provide further evidence of a radical-coupling mechanism, ESR spectra were acquired on the mixture of PANI powder and different amounts of the MgS_x catholyte. The intensity and the peak position of each ESR signal were found to be altered with the increasing amount of the MgS_x catholyte, as represented in Figure 3b. The gradual suppression of the ESR signal intensity and the shift in peak position with a characteristic broader line width strongly corroborate the plausible adduct formation between PANI and the $S_3^{\bullet-}$ species through radical coupling. The shift in peak position and the broadening of the ESR signal width could be attributed to changes in the chemical environment due to adduct formation. To further understand the catalytic activity of polyaniline on the electrochemical conversion of

https://doi.org/10.1021/acs.jpclett.1c04021
J. Phys. Chem. Lett. 2022, 13, 1337−1343

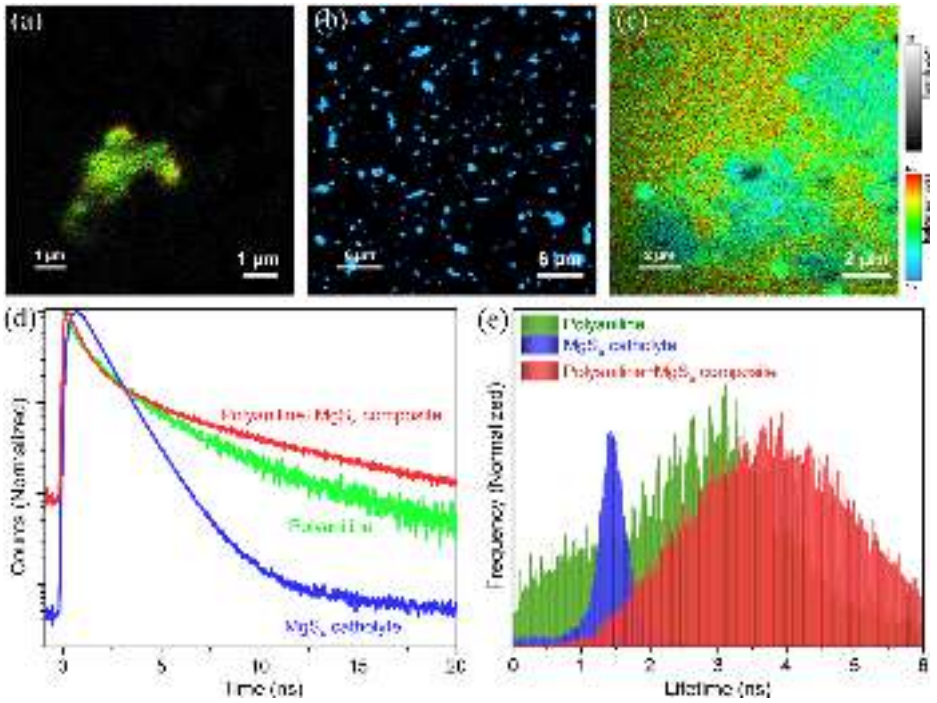

Figure 4. Fluorescence lifetime images of films of polyaniline (a), MgS_x (b), and polyaniline/MgS_x composite (c) recorded using an excitation wavelength (λ_{ex}) of 405 nm and their corresponding bulk photoluminescence transients (d) and lifetime distributions (e).

higher-order Mg-polysulfides (MgS_x, $8 \geq x \geq 4$) to lower-order Mg-sulfides (MgS_n, $2 \geq n \geq 1$), S(2p) XPS spectra were recorded on both the CC@MgS_x and CC@PANI@MgS_x electrodes after they were completely discharged to 0.5 V (vs Mg^{2+}/Mg). Deconvoluted S $2p_{3/2}$ XPS spectra of both the completely discharged electrodes exhibit the characteristic peaks of both higher-order Mg-polysulfides and lower-order Mg-sulfides[14] (Figure 3c,d). However, it is noteworthy to observe that the relative peak intensity of lower-order Mg-sulfides is higher for the CC@PANI@MgS_x cathode (Figure 3c), indicating a larger extent of electrochemical conversion of MgS_x to end-discharge products. We propose that polyaniline (PANI) anchors $S_3^{\bullet-}$ species from the catholyte through a radical-coupling mechanism to form a chemical adduct, which expedites electron transfer from the current collector that causes successive reduction of the $S_3^{\bullet-}$ moiety to form MgS_2 and eventually MgS as the end-discharge products.

Free radicals present in polyaniline and MgS_x polysulfide were further characterized using fluorescence spectroscopy. Emission spectra of polyaniline and MgS_x are shown in Figure S4. Fluorescence lifetime images of individual polyaniline and MgS_x were compared with the those of MgS_x adsorbed polyaniline sample (Figure 4a−c). The lifetime of polyaniline is found to be triexponential with the values of 0.59 ns (50%), 2.04 ns (38%), and 5.2 ns (12%) (Figure 4d and Table S1), which are similar to the reported literature values.[33,34] In comparison to polyaniline, the MgS_x sample has a much smaller lifetime of ∼1.3 ns. This indicates the high possibility of cross-coupling between polyaniline and MgS_x.[35] The MgS_x adsorbed polyaniline exhibited a longer lifetime than polyaniline and MgS_x individuals. Moreover, both the characteristic photoluminescence transient and lifetime distributions of MgS_x adsorbed polyaniline closely resemble those of polyaniline, suggesting an obvious modification in the chemical environment of polyaniline possibly due to radical-coupling interactions with polysulfur radical-anions present in MgS_x and corresponding adduct formation.

In summary, as schematically illustrated in Figure S5, during discharge of a Mg/S battery containing the CC@PANI@MgS_x cathode, the low-concentrated MgS_x catholyte generates a relatively stable $S_3^{\bullet-}$ radical-monoanion through an entropy-driven homolytic bond dissociation (i.e., disproportionation) of higher-order polysulfides and quickly achieves a dynamic equilibrium. Subsequently, electron spin resonance spectra characterization and fluorescence lifetime measurements indicate that polyaniline (more specifically polysemiquinone radical-cations) anchor the $S_3^{\bullet-}$ species from the MgS_x catholyte through a free-radical-coupling process, which might facilitate electron transfer from the substrate that leads to further reduction of $Mg(S_3^{\bullet-})_2$ to form MgS_2 and eventually to MgS as the end-discharged product. Formation of the mixed-phase end-discharged product of MgS_2 and MgS is confirmed by X-ray photoelectron spectroscopy. The rapid electrochemical conversion of $Mg(S_3^{\bullet-})_2$ to lower-order Mg-sulfides (MgS_2/MgS) by polyaniline might expedite the disproportionation process of higher-order polysulfides in order to maintain the dynamic equilibrium. Therefore, we hypothesize that the prominent redox peaks, observed in the cyclic voltammogram of the CC@PANI@MgS_x cathode, are due to the rapid disproportionation of higher-order polysulfides to $S_3^{\bullet-}$ radical-anions as well as subsequent electrochemical reduction of the $S_3^{\bullet-}$ moiety to the lower-order Mg-sulfides by polyaniline.

In conclusion, magnesium−sulfur (Mg−S) batteries achieving high specific capacity and stable cyclability have been practically realized using polyaniline-coated carbon cloth as a current collector. The superior electronic conductivity of polyaniline increases the utilization of active material, while the hydrophilic nature of polyaniline helps to immobilize and retain the electrolyte-soluble intermediates in the cathode.

https://doi.org/10.1021/acs.jpclett.1c04021
J. Phys. Chem. Lett. 2022, 13, 1337−1343

Electron spin resonance spectroscopy and X-ray photoelectron spectroscopy characterization reveal that polyaniline catalyzes the electrochemical conversion of high-order Mg-polysulfides to the end-discharge products through formation of a chemical adduct between polyaniline and MgS_x, as further indicated by fluorescence lifetime measurements. The design of such a hybrid current collector with electrocatalytic properties, as demonstrated hereby, will open a new direction to enhance the overall electrochemical performance of the Mg/S batteries.

■ ASSOCIATED CONTENT

Supporting Information

The Supporting Information is available free of charge at https://pubs.acs.org/doi/10.1021/acs.jpclett.1c04021.

Experimental methods, XPS and SEM images of CC@PANI, Raman and UV−visible spectrum of the MgS_x catholyte, discharge profile of CC@PANI@MgS_x, photoluminescence spectra of polyaniline and MgS_x, fitting parameters of photoluminescence transients, and reaction mechanism schematic (PDF)

Transparent Peer Review report available (PDF)

■ AUTHOR INFORMATION

Corresponding Author

Sagar Mitra − *Electrochemical Energy Laboratory, Department of Energy Science and Engineering, Indian Institute of Technology Bombay, Mumbai 400076, India;* orcid.org/0000-0002-2604-5042; Email: sagar.mitra@iitb.ac.in

Authors

Murali Krishna − *Electrochemical Energy Laboratory, Department of Energy Science and Engineering, Indian Institute of Technology Bombay, Mumbai 400076, India*

Arnab Ghosh − *Electrochemical Energy Laboratory, Department of Energy Science and Engineering, Indian Institute of Technology Bombay, Mumbai 400076, India*

Divyamahalakshmi Muthuraj − *Electrochemical Energy Laboratory, Department of Energy Science and Engineering, Indian Institute of Technology Bombay, Mumbai 400076, India*

Sharmistha Das − *Department of Chemistry, Indian Institute of Technology Bombay, Mumbai 400076, India*

Complete contact information is available at: https://pubs.acs.org/10.1021/acs.jpclett.1c04021

Author Contributions

M.K., A.G., and S.M. conceived the idea of this work and discussed all the experimental data. M.K., A.G., and D.M. designed the research framework and undertook materials synthesis, physical characterization, and electrochemical experiments. M.K., A.G., and S.D. performed photoluminescence lifetime measurement experiments and analyzed the data. The manuscript was written by M.K., A.G., and S.M. with the aid of all authors. S.M. supervised the project.

Notes

The authors declare no competing financial interest.

■ ACKNOWLEDGMENTS

This work is supported by the Department of Science and Technology (DST), Govt. of India, as a special call on Materials for Energy Storage (MES) (grant no DST/TMD/MES/2K17/66). We also thank the National Centre for Solar Photovoltaic Research and Education (NCPRE), funded by the Ministry of New and Renewable Energy, Govt. of India, the Indian Institute of Technology Bombay. The authors are thankful to SAIF IIT Bombay and IRCC IIT Bombay for the analysis support.

■ REFERENCES

(1) Kim, H. S.; Arthur, T. S.; Allred, G. D.; Zajicek, J.; Newman, J. G.; Rodnyansky, A. E.; Oliver, A. G.; Boggess, W. C.; Muldoon, J. Structure and Compatibility of a Magnesium Electrolyte with a Sulphur Cathode. *Nat. Commun.* **2011**, *2*, 427.

(2) Jäckle, M.; Groß, A. Microscopic Properties of Lithium, Sodium, and Magnesium Battery Anode Materials Related to Possible Dendrite Growth. *J. Chem. Phys.* **2014**, *141*, 174710.

(3) Wang, P.; Buchmeiser, M. R. Rechargeable Magnesium−Sulfur Battery Technology: State of the Art and Key Challenges. *Adv. Funct. Mater.* **2019**, *29*, 1905248.

(4) Kong, L.; Yan, C.; Huang, J.-Q.; Zhao, M.-Q.; Titirici, M.-M.; Xiang, R.; Zhang, Q. A Review of Advanced Energy Materials for Magnesium−Sulfur Batteries. *Energy Environ. Mater.* **2018**, *1*, 100−112.

(5) Zhao-Karger, Z.; Liu, R.; Dai, W.; Li, Z.; Diemant, T.; Vinayan, B. P.; Minella, C. B.; Yu, X.; Manthiram, A.; Behm, R. J.; Ruben, M.; Fichtner, M. Toward Highly Reversible Magnesium−Sulfur Batteries with Efficient and Practical $Mg[B(hfip)_4]_2$ Electrolyte. *ACS Energy Lett.* **2018**, *3*, 2005−2013.

(6) Zhao-Karger, Z.; Zhao, X.; Wang, D.; Diemant, T.; Behm, R. J.; Fichtner, M. Performance Improvement of Magnesium Sulfur Batteries with Modified Non-Nucleophilic Electrolytes. *Adv. Energy Mater.* **2015**, *5*, 1401155.

(7) Gao, T.; Noked, M.; Pearse, A. J.; Gillette, E.; Fan, X.; Zhu, Y.; Luo, C.; Suo, L.; Schroeder, M. A.; Xu, K.; Lee, S. B.; Rubloff, G. W.; Wang, C. Enhancing the Reversibility of Mg/S Battery Chemistry through Li^+ Mediation. *J. Am. Chem. Soc.* **2015**, *137*, 12388−12393.

(8) Zhang, Z.; Cui, Z.; Qiao, L.; Guan, J.; Xu, H.; Wang, X.; Hu, P.; Du, H.; Li, S.; Zhou, X.; Dong, S.; Liu, Z.; Cui, G.; Chen, L. Novel Design Concepts of Efficient Mg-Ion Electrolytes toward High-Performance Magnesium−Selenium and Magnesium−Sulfur Batteries. *Adv. Energy Mater.* **2017**, *7*, 1602055.

(9) Ha, S.-Y.; Lee, Y.-W.; Woo, S. W.; Koo, B.; Kim, J.-S.; Cho, J.; Lee, K. T.; Choi, N.-S. Magnesium(II) Bis(Trifluoromethane Sulfonyl) Imide-Based Electrolytes with Wide Electrochemical Windows for Rechargeable Magnesium Batteries. *ACS Appl. Mater. Interfaces* **2014**, *6*, 4063−4073.

(10) Li, W.; Cheng, S.; Wang, J.; Qiu, Y.; Zheng, Z.; Lin, H.; Nanda, S.; Ma, Q.; Xu, Y.; Ye, F.; Liu, M.; Zhou, L.; Zhang, Y. Synthesis, Crystal Structure, and Electrochemical Properties of a Simple Magnesium Electrolyte for Magnesium/Sulfur Batteries. *Angew. Chemie Int. Ed.* **2016**, *55*, 6406−6410.

(11) Vinayan, B. P.; Zhao-Karger, Z.; Diemant, T.; Chakravadhanula, V. S. K.; Schwarzburger, N. I.; Cambaz, M. A.; Behm, R. J.; Kübel, C.; Fichtner, M. Performance Study of Magnesium−Sulfur Battery Using a Graphene Based Sulfur Composite Cathode Electrode and a Non-Nucleophilic Mg Electrolyte. *Nanoscale* **2016**, *8*, 3296−3306.

(12) Zhou, X.; Tian, J.; Hu, J.; Li, C. High Rate Magnesium−Sulfur Battery with Improved Cyclability Based on Metal−Organic Framework Derivative Carbon Host. *Adv. Mater.* **2018**, *30*, 1704166.

(13) Muthuraj, D.; Ghosh, A.; Kumar, A.; Mitra, S. Nitrogen and Sulfur Doped Carbon Cloth as Current Collector and Polysulfide Immobilizer for Magnesium-Sulfur Batteries. *ChemElectroChem.* **2019**, *6*, 684−689.

(14) Muthuraj, D.; Pandey, M.; Krishna, M.; Ghosh, A.; Sen, R.; Johari, P.; Mitra, S. Magnesium Polysulfide Catholyte (MgS_x): Synthesis, Electrochemical and Computational Study for Magnesium-Sulfur Battery Application. *J. Power Sources* **2021**, *486*, 229326.

(15) Wang, P.; Xi, B.; Huang, M.; Chen, W.; Feng, J.; Xiong, S. Emerging Catalysts to Promote Kinetics of Lithium−Sulfur Batteries. *Adv. Energy Mater.* **2021**, *11*, 2002893.
(16) Gao, W.; Wang, Z.; Peng, C.; Kang, S.; Cui, L. Accelerating the Redox Kinetics by Catalytic Activation of "Dead Sulfur" in Lithium−Sulfur Batteries. *J. Mater. Chem. A* **2021**, *9*, 13442−13458.
(17) He, J.; Manthiram, A. A Review on the Status and Challenges of Electrocatalysts in Lithium-Sulfur Batteries. *Energy Storage Mater.* **2019**, *20*, 55−70.
(18) Huang, X. L.; Wang, Y.-X.; Chou, S.-L.; Dou, S. X.; Wang, Z. M. Materials Engineering for Adsorption and Catalysis in Room-Temperature Na−S Batteries. *Energy Environ. Sci.* **2021**, *14*, 3757−3795.
(19) Amaya, T.; Kurata, I.; Inada, Y.; Hatai, T.; Hirao, T. Synthesis of Phosphonic Acid Ring-Substituted Polyanilines via Direct Phosphonation to Polymer Main Chains. *RSC Adv.* **2017**, *7*, 39306−39313.
(20) Nobrega, M. M.; Izumi, C. M. S.; Temperini, M. L. A. Probing Molecular Ordering in the HCl-Doped Polyaniline with Bulk and Nanofiber Morphology by Their Thermal Behavior. *Polym. Degrad. Stab.* **2015**, *113*, 66−71.
(21) Silva, C. H. B.; Da Costa Ferreira, A. M.; Constantino, V. R. L.; Temperini, M. L. A. Hybrid Materials of Polyaniline and Acidic Hexaniobate Nanoscrolls: High Polaron Formation and Improved Thermal Properties. *J. Mater. Chem. A* **2014**, *2*, 8205−8214.
(22) Huang, W. S.; MacDiarmid, A. G. Optical Properties of Polyaniline. *Polymer* **1993**, *34*, 1833−1845.
(23) Nobrega, M. M.; Martins, V. L.; Torresi, R. M.; Temperini, M. L. A. One-Step Synthesis, Characterization, and Properties of Emeraldine Salt Nanofibers Containing Gold Nanoparticles. *J. Phys. Chem. C* **2014**, *118*, 4267−4274.
(24) Pereira da Silva, J. E.; De Faria, D. L. A.; De Torresi, S. I.; Temperini, M. L. A. Influence of Thermal Treatment on Doped Polyaniline Studied by Resonance Raman Spectroscopy. *Macromolecules* **2000**, *33*, 3077−3083.
(25) Scherr, E. M.; MacDiarmid, A. G.; Manohar, S. K.; Masters, J. G.; Sun, Y.; Tang, X.; Druy, M. A.; Glatkowski, P. J.; Cajipe, V. B.; Fischer, J. E.; Cromack, K. R.; Jozefowicz, M. E.; Ginder, J. M.; McCall, R. P.; Epstein, A. J. Polyaniline: Oriented Films and Fibers. *Synth. Met.* **1991**, *41*, 735−738.
(26) Vijayakumar, M.; Govind, N.; Walter, E.; Burton, S. D.; Shukla, A.; Devaraj, A.; Xiao, J.; Liu, J.; Wang, C.; Karim, A.; Thevuthasan, S. Molecular Structure and Stability of Dissolved Lithium Polysulfide Species. *Phys. Chem. Chem. Phys.* **2014**, *16*, 10923−10932.
(27) Wang, Q.; Zheng, J.; Walter, E.; Pan, H.; Lv, D.; Zuo, P.; Chen, H.; Deng, Z. D.; Liaw, B. Y.; Yu, X.; Yang, X.; Zhang, J.-G.; Liu, J.; Xiao, J. Direct Observation of Sulfur Radicals as Reaction Media in Lithium Sulfur Batteries. *J. Electrochem. Soc.* **2015**, *162*, A474−A478.
(28) Wujcik, K. H.; Wang, D. R.; Raghunathan, A.; Drake, M.; Pascal, T. A.; Prendergast, D.; Balsara, N. P. Lithium Polysulfide Radical Anions in Ether-Based Solvents. *J. Phys. Chem. C* **2016**, *120*, 18403−18410.
(29) Kumar, A.; Ghosh, A.; Forsyth, M.; MacFarlane, D. R.; Mitra, S. Free-Radical Catalysis and Enhancement of the Redox Kinetics for Room-Temperature Sodium−Sulfur Batteries. *ACS Energy Lett.* **2020**, *5*, 2112−2121.
(30) Vinayan, B. P.; Euchner, H.; Zhao-Karger, Z.; Cambaz, M. A.; Li, Z.; Diemant, T.; Behm, R. J.; Gross, A.; Fichtner, M. Insights into the Electrochemical Processes of Rechargeable Magnesium−Sulfur Batteries with a New Cathode Design. *J. Mater. Chem. A* **2019**, *7*, 25490−25502.
(31) Lu, X.; Kirby, B. W.; Xu, W.; Li, G.; Kim, J.; Lemmon, J.; Sprenkle, V.; Yang, Z. Advanced Intermediate-Temperature Na-S Battery. *Energy Environ. Sci.* **2013**, *6*, 299−306.
(32) Yeon, J.-T.; Jang, J.-Y.; Han, J.-G.; Cho, J.; Lee, K. T.; Choi, N.-S. Raman Spectroscopic and X-Ray Diffraction Studies of Sulfur Composite Electrodes during Discharge and Charge. *J. Electrochem. Soc.* **2012**, *159*, A1308−A1314.
(33) Saha, P.; Pyne, D. K.; Pal, M.; Datta, S.; Das, P. K.; Dutta, P.; Halder, A. pH Dependent Tunable Photoluminiscence of Polyaniline Grafted Graphene Oxide (GO-PANI) Nanocomposite. *J. Lumin.* **2017**, *181*, 138−146.
(34) Pandiyarajan, T.; Mangalaraja, R. V.; Karthikeyan, B. Enhanced Ultraviolet Fluorescence in Surface Modified ZnO Nanostructures: Effect of PANI. *Spectrochim. Acta A Mol. Biomol. Spectrosc.* **2015**, *147*, 280−285.
(35) Sohtome, Y.; Kanomata, K.; Sodeoka, M. Cross-Coupling Reactions of Persistent Tertiary Carbon Radicals. *Bull. Chem. Soc. Jpn.* **2021**, *94*, 1066−1079.

https://doi.org/10.1021/acs.jpclett.1c04021
J. Phys. Chem. Lett. 2022, 13, 1337−1343